Monthly Notices
of the
ROYAL ASTRONOMICAL SOCIETY

MNRAS **490,** 1–8 (2019)
Advance Access publication 2019 September 16

doi:10.1093/mnras/stz2574

A fast radio burst in the direction of the Virgo Cluster

Devansh Agarwal ,[1,2]★ Duncan R. Lorimer,[1,2] Anastasia Fialkov,[3,4,5] Keith W. Bannister,[6] Ryan M. Shannon,[7] Wael Farah,[7] Shivani Bhandari,[6] Jean-Pierre Macquart ,[8] Chris Flynn,[7] Giuliano Pignata,[9,10] Nicolas Tejos,[11] Benjamin Gregg,[8] Stefan Osłowski ,[7] Kaustubh Rajwade ,[12] Mitchell B. Mickaliger,[12] Benjamin W. Stappers,[12] Di Li ,[13,14] Weiwei Zhu,[13] Lei Qian,[13] Youling Yue,[13] Pei Wang[13] and Abraham Loeb[15]

[1]*Department of Physics and Astronomy, West Virginia University, PO Box 6315, Morgantown, WV 25606, USA*
[2]*Center for Gravitational Waves and Cosmology, West Virginia University, Chestnut Ridge Research Building, Morgantown, WV 26505, USA*
[3]*Kavli Institute for Cosmology, University of Cambridge, Madingley Road, Cambridge CB3 0HA, UK*
[4]*Institute of Astronomy, University of Cambridge, Madingley Road, Cambridge CB3 0HA, UK*
[5]*Department of Physics and Astronomy, University of Sussex, Falmer, Brighton BN1 9QH, UK*
[6]*CSIRO Astronomy and Space Science, Australia Telescope National Facility, Box 76, Epping, NSW 1710, Australia*
[7]*Centre for Astrophysics and Supercomputing, Swinburne University of Technology, Hawthorn, VIC 3122, Australia*
[8]*Department of Astronomy, University of Massachusetts Amherst, Amherst, MA 01002, USA*
[9]*Departamento de Ciencias Fisicas, Universidad Andres Bello, Avda. Republica 252, Santiago, Chile*
[10]*Millennium Institute of Astrophysics (MAS), Nuncio Monseñor Sotero Sanz 100, Providencia, Santiago, Chile*
[11]*Instituto de Física, Pontificia Universidad Católica de Valparaíso, Casilla 4059, Valparaíso, Chile*
[12]*Jodrell Bank Centre for Astrophysics, University of Manchester, Oxford Road, Manchester M13 9PL, UK*
[13]*CAS Key Laboratory of FAST, National Astronomical Observatories, Chinese Academy of Sciences, Beijing 10010, China*
[14]*NAOC-UKZN Computational Astrophysics Centre, University of KwaZulu-Natal, Durban 4000, South Africa*
[15]*Astronomy Department, Harvard University, 60 Garden St, Cambridge, MA 02138, USA*

Accepted 2019 September 11. Received 2019 September 9; in original form 2019 June 26

ABSTRACT

The rate of fast radio bursts (FRBs) in the direction of nearby galaxy clusters is expected to be higher than the mean cosmological rate if intrinsically faint FRBs are numerous. In this paper, we describe a targeted search for faint FRBs near the core of the Virgo Cluster using the Australian Square Kilometre Array Pathfinder telescope. During 300 h of observations, we discovered one burst, FRB 180417, with dispersion measure (DM) = 474.8 cm^{-3} pc. The FRB was promptly followed up by several radio telescopes for 27 h, but no repeat bursts were detected. An optical follow-up of FRB 180417 using the PROMPT5 telescope revealed no new sources down to an *R*-band magnitude of 20.1. We argue that FRB 180417 is likely behind the Virgo Cluster as the Galactic and intracluster DM contribution are small compared to the DM of the FRB, and there are no galaxies in the line of sight. The non-detection of FRBs from Virgo constrains the faint-end slope, $\alpha < 1.52$ (at 68 per cent confidence limit), and the minimum luminosity, $L_{\rm min} \gtrsim 2 \times 10^{40}$ erg s^{-1} (at 68 per cent confidence limit), of the FRB luminosity function assuming cosmic FRB rate of 10^4 FRBs per sky per day with flux above 1 Jy located out to redshift of 1. Further FRB surveys of galaxy clusters with high-sensitivity instruments will tighten the constraints on the faint end of the luminosity function and, thus, are strongly encouraged.

Key words: surveys – radio continuum: general.

1 INTRODUCTION

Fast radio bursts (FRBs) are extremely bright, highly dispersed pulses of as yet unknown origin. Following the serendipitous discovery of the prototypical 'Lorimer burst' in archival pulsar search

★ E-mail: da0017@mix.wvu.edu

data (Lorimer et al. 2007), FRBs were subsequently confirmed as a cosmological population in dedicated surveys (Thornton et al. 2013) and now over ∼90 sources are known (Petroff et al. 2016).[1] Notable discoveries also include the 11 repeating sources: FRB 121102 (Spitler et al. 2016), nine sources reported by The CHIME/FRB Collaboration et al. (2019a,b), and FRB 1701019 (Kumar et al. 2019). While many theories have been proposed (for a recent compilation, see Platts et al. 2019), the origin of both repeating and non-repeating FRBs is still a mystery.

While on-going blind large-area surveys are providing valuable insights into the population (James et al. 2018; Shannon et al. 2018; James 2019), targeted searches can also prove fruitful. Recently, in one such attempt to optimize searches, Fialkov, Loeb & Lorimer (2018) predict a possible enhancement in the FRB rate in the direction of nearby galaxy clusters if the intrinsically faint FRB population is abundant. Their study was motivated by the availability of small (∼20 m class) radio telescopes that often have large amounts of observing time available with a modest (∼1 deg^2) field of view, but it can also be investigated by facilities with broader sky coverage. Motivated by these predictions, and the great success of the Australian Square Kilometre Array Pathfinder (ASKAP; Schinckel et al. 2012) in finding FRBs (Bannister et al. 2017; Shannon et al. 2018), we have conducted a 300-h survey with ASKAP to look for such an excess in the direction of the Virgo galaxy cluster.

The search was successful in that we found one new FRB 180417 ∼3° away from the cluster centre. In this paper, we describe the survey observations and the properties of this new FRB in Section 2. We also summarize the follow-up observations for repeat bursts in Section 3. In Section 4, we comment on its possible location behind the Virgo Cluster. We employ the non-detection of the FRB from the Virgo Cluster to derive constraints on the slope and the minimum luminosity cut-off of the FRB luminosity function at the faint end in Section 5.

2 OBSERVATIONS

The observations were carried out using the commissioning array under the Commensal Real-Time ASKAP Fast-Transients (CRAFT) survey (Macquart et al. 2010). Depending on availability we used 6–8 ASKAP antennas in the incoherent summed mode. The observations were carried out from 2018 March 9 to 2018 May 9, with approximately 7 h d^{-1}. The field centre is right ascension (RA) 12^{h}33^m and declination (Dec.) +13°34′ in the J2000 epoch. These coordinates were reported by Fialkov et al. (2018) for the maximum FRB rates from Virgo. Fig. 1 shows the ASKAP footprint overlaid on a *ROSAT* image of the cluster (Truemper 1982). The data capturing pipeline is detailed in Bannister et al. (2017). Total intensity streams from 36 beams of each antenna were recorded on the disc and summed offline. The data were then searched for FRBs using the identical pipeline as described in Bannister et al. (2017). We use the graphics processing unit accelerated real-time search pipeline FREDDA (Bannister et al., in preparation) and search for 12 different pulse widths in the range 1.26–15.12 ms over a dispersion measure (DM) interval of 20–4096 cm^{-3} pc. Candidates were clustered together using the friends-of-friends (FoF) algorithm (Huchra & Geller 1982) and archived along with their maximum signal-to-noise ratio (S/N). Clustered candidates with S/N > 10 were selected for subsequent visual inspection.

[1] http://www.frbcat.org

3 RESULTS

One FRB was detected as a result of these observations and data processing, FRB 180417. We detail the parameters of this source and the follow-up observations we carried out in the subsections below.

3.1 FRB 180417

FRB 180417 was strongly detected in three beams with S/N > 14, and further in two beams with S/N > 5, as shown in Table 1.

Fig. 2 shows the frequency versus time plot with S/N = 24.2 from the co-addition of these beams. The pulse was detectable at S/N ∼ 5 in individual antennas with similar frequency structure.

The estimated Galactic DM contribution in the direction of the FRB using NE2001 (Cordes & Lazio 2002, 2003) and YMW16 (Yao, Manchester & Wang 2017) is 26.15 and 20.39 pc cm^{-3}, respectively. We estimate the Galactic halo DM contribution to be ≈30 pc cm^{-3} (see Dolag et al. 2015 and Section 4.1 for more discussion). Properties of the FRB are summarized in Table 2. The multiple-beam detections of FRB 180417 allow us to constrain the burst location and fluence. To do so, we use the method described in detail in section 4.1 of Bannister et al. (2017) that we summarize here. Using a model for the responses for adjacent beams, we use the beam positions on the sky and burst S/N to infer the burst position and attenuation. The position and attenuation are inferred using Bayesian methodology, after accounting for uncertainties in beam gain, shape, and position. The method has been found to be robust in bursts with the position derived for FRB 180924 using this method consistent with the interferometric position (Bannister et al. 2019), and with the detection of repeat pulses of ASKAP FRB 171019 with the Green Bank Telescope (Kumar et al. 2019). Using the positions and S/N for the beams around the FRB 180417 detection (see Table 1), we are able to constrain the location to an error box of size 7 × 7 arcmin^2 and the fluence as 55 ± 3 Jy ms.

We characterize the spectral variations by computing the mean normalized autocorrelation function of the spectrum (f_ν) as

$$\xi(\Delta\nu) = \frac{\left\langle [f_\nu(\nu' + \Delta\nu) - \bar{f}_\nu][f_\nu(\nu') - \bar{f}_\nu] \right\rangle}{\bar{f}_\nu^2}. \quad (1)$$

Here $\bar{f}_\nu$ is the mean spectrum amplitude. Fig. 3 shows the autocorrelation function of the FRB spectra. We fit the above with $\xi(\Delta\nu) = m/(f_{\rm dc}^2 + \Delta\nu^2)$ and obtain a decorrelation bandwidth, $f_{\rm dc} = 4.3 \pm 0.4$ MHz and the modulation index, $m = 0.47 \pm 0.07$ (Cordes 1986). This is consistent with expectation for the interstellar medium (ISM) at this location on the sky based on the NE2001 model. The NE2001 model estimates $f_{\rm dc,\,NE2001} = 6.3$ MHz at 1.4 GHz, implying the ISM is responsible for the spectral variations.

3.2 Radio follow-up observations

We have undertaken an extensive follow-up campaign to search for repetition from FRB 180417. Owing to the nature of our survey, we have repeatedly covered the region of FRB 180417. The FRB was discovered when 53 per cent of our 300 h survey was completed. We have spent a total of 27.1 h searching at the location of the burst with other telescopes as detailed below.

Starting soon after the detection, we began following up using various other telescopes. The most rapid follow-up occurred with the Parkes and Lovell radio telescopes that were able to perform a search for repeated bursts within 24 h of the original detection, with the Five-hundred-meter Aperture Spherical radio Telescope

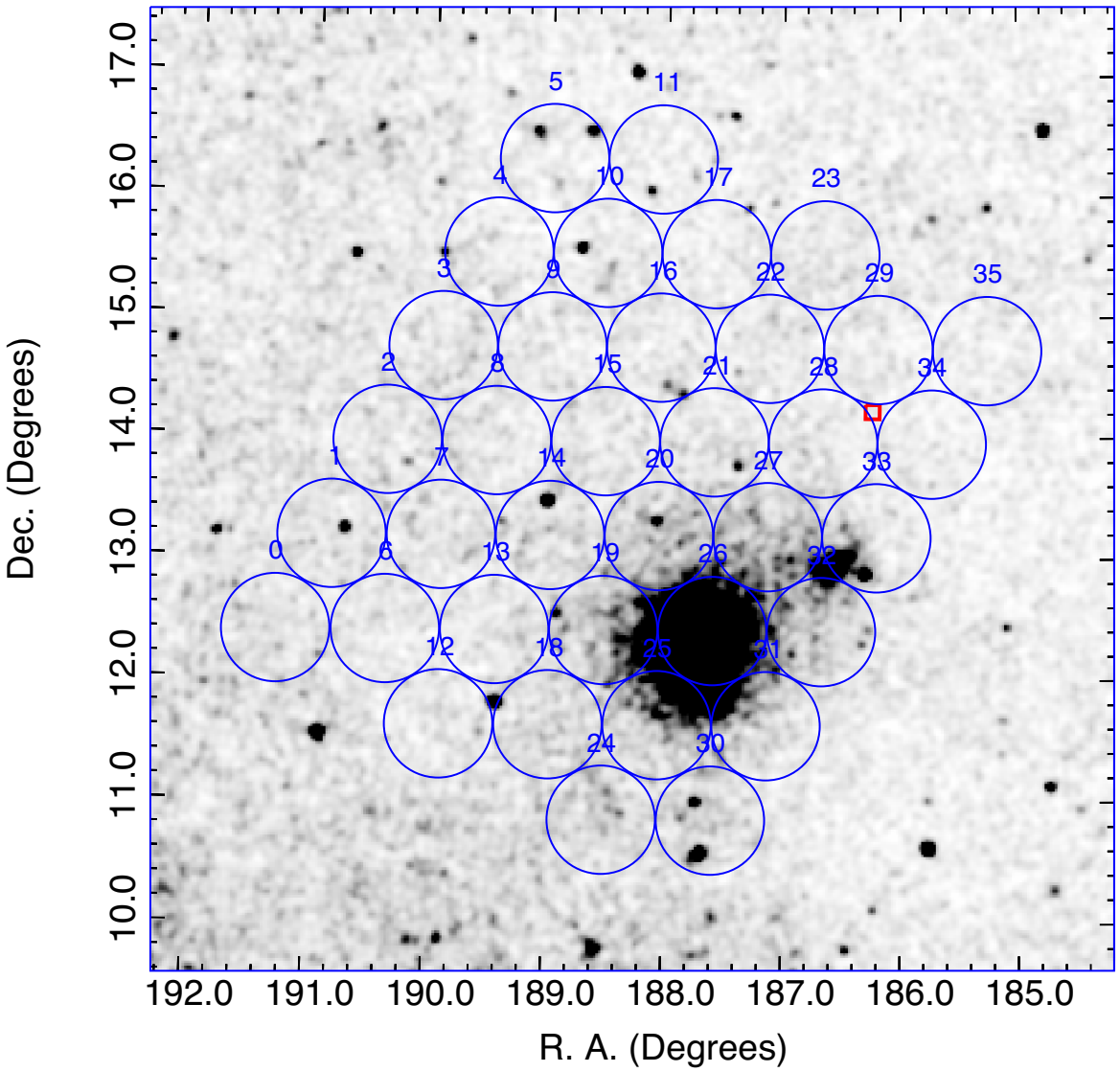

Figure 1. The ASKAP footprint overlaid on the *ROSAT* All-Sky Survey grey-scale image of the Virgo Cluster of galaxies. The red box denotes the location of FRB 180417. The dark region near Beam 26 is dominated by M87, a giant elliptical galaxy at the centre of the Virgo Cluster.

Table 1. Detection S/N of FRB 180417.

Beam	RA (J2000)	Dec. (J2000)	S/N
21	12:30:20	13:58:07	0.6
22	12:28:28	14:44:48	5.4
27	12:28 30	13:11:15	3.0
28	12:26:38	13:57:52	15.0
29	12:24:45	14:44:25	16.8
33	12:24:48	13:10:44	5.9
34	12:22:55	13:57:24	14.0

(FAST) and a 20-m dish at the Green Bank Observatory joining soon after. The advantage of the follow-up using larger telescopes is the increased sensitivity that is beneficial as we expect there would be weaker bursts, in line with the observed properties of FRB 121102. Under our follow-up, FAST was the most sensitive telescope with 0.03 Jy ms fluence limit (Nan et al. 2011; Li et al. 2018). The data were searched for DM range or 400–550 pc cm^{-3} with 1000 trials using HEIMDALL.[2] Candidates with S/N > 6 were inspected visually. Table 3 describes the follow-up details. We did not detect any repeat bursts, and we defer detailed limits and modelling to a separate publication.

3.3 Optical follow-up

Optical imaging at the location of the FRB 180417 (red cross in Fig. 4) was carried out on 2018 May 11.96 UT with the 40-cm PROMPT5 telescope located at Cerro Tololo Inter-American Observatory (CTIO). PROMPT5 has a field of view of 11 × 11 arcmin^2 fully covering the position uncertainty derived by the ASKAP observations (green box in Fig. 4). A series of thirty 40-s *R*-band images were acquired for a total integration time of 20 min. Each frame was correct for bias, dark, and flat using standard routines in IRAF. A final image was obtained taking a median value for each

[2]https://sourceforge.net/projects/heimdall-astro

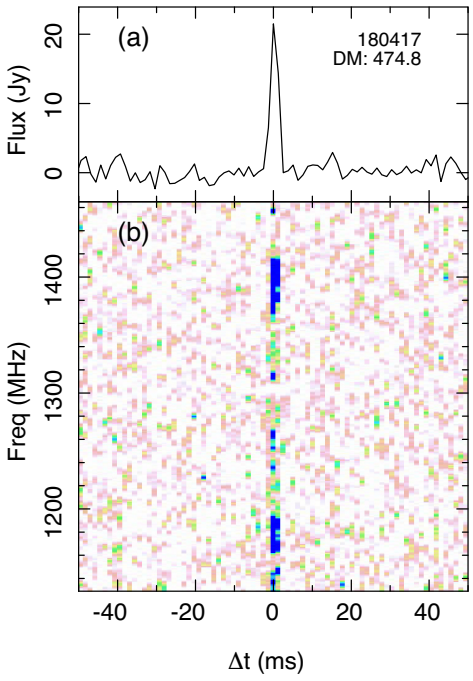

Figure 2. The dedispersed profile and dynamic spectrum for FRB 180417. The top panel shows the co-added profile from all three beams. The bottom panel shows the dynamic spectrum of the FRB. The frequency structure of the FRB is clumpy that is similar to previously reported FRBs from ASKAP (Macquart et al. 2019).

Table 2. Observed properties of FRB 180417.

Parameter	Value
UTC	2018-04-17 13:18:31 (at 1297 MHz)
MJD	58225.55452546
S/N	24.2
DM	474.8 pc cm^{-3}
RA (J2000)	$12^{h}24^{m}56(28)^{s}$
Dec. (J2000)	$+14^{\circ}13(7)'$
Boxcar width	2.52 ms
Fluence	55(3) Jy ms

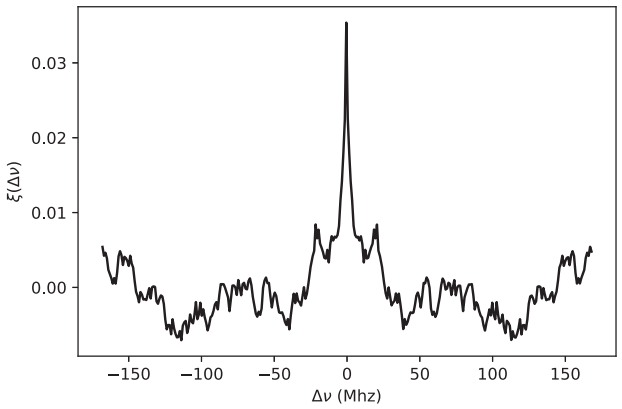

Figure 3. The autocorrelation function of the spectrum of FRB 180417.

Table 3. Details of the radio follow-up of FRB 180417. Here F_{min} is the minimum fluence detectable by the telescope.

Telescope	Observation length (h)	F_{min} (Jy ms)
GB 20-m	16.0	4.8
FAST	0.5	0.03
Parkes	6.6	2.0
Lovell	4.0	0.5

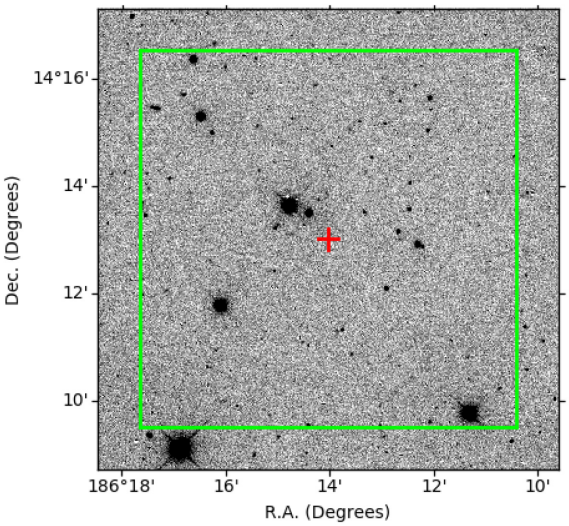

Figure 4. PROMPT5 image acquired on 2018 May 11.96 UT. The red cross indicates the FRB 180417 position, while the green square shows the corresponding error box.

pixel. The photometry was calibrated using the magnitude of stars present in the PROMPT field of view, reported in the Panoramic Survey Telescope And Rapid Response System (Pan-STARRS) photometric catalogue (Magnier et al. 2016) transformed to the Johnson–Kron Cousins photometric system using the transformation reported in Smith et al. (2002).

To search for an optical counterpart of FRB 180417, we searched optical archives looking for images obtained before the FRB occurrence. In the Canada–France–Hawaii Telescope (CFHT) archive we found an *r*-band MegaCam image with a total integration time of 1374 s acquired on 2013 May 14, which fully covered the PROMPT5 image. We aligned, rescaled, and convolved the MegaCam image with SWarp (Bertin et al. 2002) and hotpants (Becker 2015) in order to match the orientation, flux, and point spread function (PSF) of the PROMPT5 frame.

In the template subtracted image, we searched for transients using algorithms developed for the CHASE survey (Pignata et al. 2009). We did not detect any source with S/N > 3. Using artificial stars placed around the FRB 180417 position, we set an upper limit of $R = 20.1$ on the optical counterpart detection. The small blank regions in the MegaCam mosaic are covered by one of the subframes of a *R*-band VMOS image acquired on 2009 February 26, we found in the ESO archive, which has an integration time of 180 s. We use the latter image as a template in the same way we did for the MegaCam frame, however, no sources with S/N > 3 were detected.

4 IMPLICATIONS OF FRB 180417

4.1 Is FRB 180417 in the Virgo Cluster?

To estimate the distance of the FRB we perform a simple analysis in which the DM of FRB 180417, $\mathrm{DM_{FRB}}$, is represented as the sum of contributions from the Milky Way (MW), intracluster medium (ICM), intergalactic medium (IGM), and the host, as follows:

$$\mathrm{DM_{FRB}} = \mathrm{DM_{MW}} + \mathrm{DM_{ICM}} + \mathrm{DM_{IGM}} + \mathrm{DM_{host}}. \quad (2)$$

Using two different Galactic electron density models NE2001 (Cordes & Lazio 2002; Yao et al. 2017) for this line of sight, and taking a Galactic halo contribution of 30 $\mathrm{cm^{-3}}$ pc, we find $\mathrm{DM_{MW}} = 60\ \mathrm{cm^{-3}}$ pc. Virgo is at a redshift of ≈0.004, and the contribution to the DM due the IGM is expected to be ≈5 $\mathrm{cm^{-3}}$ pc (using DM–redshift relation from Inoue 2004), and is considered to be negligible. We model $\mathrm{DM_{ICM}}$ from the Virgo Cluster as described below. Lastly, we leave the host galaxy contribution, $\mathrm{DM_{host}}$, as a free parameter.

Planck Collaboration XL (2016) have used X-ray and *Planck* data to estimate the electron density (n_e) out to two viral radii (2.4 Mpc) as a function of the radius. Using this model, the electron density is

$$n_\mathrm{e}(b, z_\mathrm{LOS}) = \frac{8.5 \times 10^{-5}\ \mathrm{cm^{-3}}}{(b^2 + z_\mathrm{LOS}^2)^{0.6}}. \quad (3)$$

Here, z_LOS is the depth along the line of sight (not to be confused with the redshift) and b is the impact parameter, both in Mpc. $z_\mathrm{LOS} = 0$, $b = 0$ corresponds to M87, the centre of the cluster. FRB 180417 is located 2.°3 from the centre of the cluster that corresponds to $b \sim 0.67$ Mpc corresponding to 0.55 times the virial radius. As a result, the intracluster contribution is

$$\begin{aligned}\mathrm{DM_{ICM}} &= 10^6\ \mathrm{cm^{-3}\ pc} \int_{-2.4}^{2.4} n_\mathrm{e}(b = 0.67, z_\mathrm{LOS})\, \mathrm{d}z_\mathrm{LOS} \\ &= 332\ \mathrm{cm^{-3}\ pc}. \end{aligned} \quad (4)$$

If FRB 180417 is indeed in the Virgo Cluster, then we can place a lower bound on the $\mathrm{DM_{host}}$ to be 90 $\mathrm{cm^{-3}}$ pc.

The location of FRB 180417 is at the outskirts of Virgo, where galaxy crowding is low. According to the Virgo catalogue (Binggeli, Sandage & Tammann 1985; Kim et al. 2014), the closest galaxy, EVCC 0548 is a dwarf spiral (dS0) galaxy, 6.3 arcmin away on the sky from the line of sight to FRB 180417 and has half-light radius of 7.5 arcsec. The next nearest galaxy is EVCC 0567, which has dwarf elliptical morphology, is 12 arcmin away from the FRB location and has half-light radius of 24 arcsec. For both of the galaxies, there are no counterparts in the NRAO VLA Sky Survey (NVSS) catalogue. Hence, it is difficult to associate the FRB with a member galaxy of Virgo.

4.2 Probing the Virgo intracluster medium

Assuming that the FRB occurred behind the Virgo Cluster, we can probe the ICM by placing constraints on scatter broadening of the pulse profile. Turbulence in the ICM would cause the radio pulse to diffract, which if sufficiently strong would cause the pulse to temporally smear. In the case of this observation, we assume that the pulse is emitted at a distance much further than the Virgo Cluster, so that we can assume the signal has a plane-parallel geometry at the Virgo Cluster. Following equation (9) from Cordes & Lazio (2002), the pulse scattering time at the distance of the Virgo Cluster (16.5 Mpc) is

$$\tau = 5.8\, \mathrm{SM}^{6/5}\, \nu^{-22/5}\ \mathrm{s}. \quad (5)$$

Here SM is the scattering measure in its conventional units of kpc $\mathrm{m^{-20/3}}$, and ν is the frequency in GHz. As the pulse width is only two bins, we assume the scatter broadening to be less than a sample, i.e. 1.26 ms. Assuming pulse scattering to be less than one sample, i.e. $\tau < 1.26$ ms, we find $\mathrm{SM} < 10^{-3.06}\ \mathrm{kpc\ m^{-20/3}}$, which can be expressed in terms of the root mean square of the electron column along the line of sight at the outer scale of the turbulence, L_0, of

$$\langle \Delta \mathrm{DM}^2 \rangle^{1/2} = 1.95 \left(\frac{L_0}{1\ \mathrm{pc}} \right)^{5/6} \mathrm{pc\,cm^{-3}}. \quad (6)$$

This limit is not strongly constraining on the scattering properties of the medium.

To place this in context, one may crudely approximate the ICM as a uniform slab of material extending out to twice the virial radius of 1.2 Mpc. This implies a limit on the *in situ* 'level of turbulence' of $C_N^2 < 3.7 \times 10^{-7}\ \mathrm{m^{-20/3}}$ (noting that the scattering measure is the integral of the level of turbulence along the ray path: $\mathrm{SM} = \int C_N^2(z)\, \mathrm{d}z$). One might plausibly expect the value of C_N^2 to be considerably lower than the limit found here for the typical plasma densities and turbulence parameters within an intracluster environment. To illustrate this point, consider a medium of mean electron density $\bar{N}_\mathrm{e}$ that gives rise to density fluctuations with variance $\langle \Delta n_\mathrm{e}^2 \rangle = \alpha^2 \bar{N}_\mathrm{e}^2$, at some outer scale L_0, plausibly of order ~ 1 kpc for the ICM. This would have a characteristic level of turbulence of

$$C_N^2 \approx 6.7 \times 10^{-9} \alpha \left(\frac{\bar{N}_\mathrm{e}}{10^{-3}\ \mathrm{cm^{-3}}} \right)^2 \left(\frac{L_0}{1\ \mathrm{kpc}} \right)^{-2/3} \mathrm{m^{-20/3}}, \quad (7)$$

where α is likely of order unity (Anantharamaiah & Narayan 1988) and we have normalized to fiducial values for an intracluster environment. Thus we observe that the present upper limit on the scattering measure, and in turn C_N^2, is still a factor of ∼50 above that might be expected in intracluster plasma.

4.3 The FRB luminosity function

Because of to the small number statistics of FRBs, their luminosity function is poorly constrained. Recently, Luo et al. (2018) used 33 FRBs from the online FRB catalogue to constrain parameters of the FRB luminosity function assuming the Schechter form so that the differential number of FRBs per unit luminosity interval is

$$\frac{\mathrm{d}N_\mathrm{FRB}}{\mathrm{d}L_\nu} \propto \left(\frac{L_\nu}{L_{\nu *}} \right)^{-\alpha} \exp\left[-\frac{L_\nu}{L_{\nu *}} \right],\ L > L_\mathrm{min}, \quad (8)$$

where α is the faint-end slope and $\nu L_{\nu *}$ is the characteristic luminosity of FRBs. The luminosity function is normalized to unity between the minimum intrinsic luminosity L_min and the maximal brightness (which we assume to be $10 L_{\nu *}$) and plays the role of the probability density of FRB luminosities. Luo et al. (2018) found the slope ranging between 1.2 and 1.8 with the best-fitting values of $\alpha \sim 1.5$ and $L_* \sim 2 \times 10^{44}$ erg $\mathrm{s^{-1}}$. From the sample, it was impossible to measure L_min due to the limited number of sources. In addition, random FRB searches typically probe mean cosmological population and pick up intrinsically brighter FRBs located at intermediate cosmological distances. For example, the 20 new FRBs recently reported by Shannon et al. (2018) were detected using ASKAP in the fly's eye mode and are probing the bright end of the luminosity function. The survey reported here is

unique in that, by surveying the nearby clustered environment of Virgo located only ∼16.5 Mpc away, ASKAP can detect faint FRBs down to $L \sim 1.3 \times 10^{39}$ erg s^{-1} that corresponds to its flux limit $S_{\rm lim,ASKAP} = 26/\sqrt{7}$ Jy. The factor of $\sqrt{7}$ is due to incoherent sum of data from (on an average) 7 antennas.

The expected FRB number counts from Virgo depend on the shape of the luminosity function, cosmic FRB event rate (used for normalization), the nature of the progenitors, and the spectral energy distribution of the bursts. In Fialkov et al. (2018) we considered two types of the luminosity function for FRBs: (i) standard candles with fixed luminosity of $\nu L_{\nu*} = 2.8 \times 10^{43}$ erg s^{-1} that corresponds to the mean intrinsic luminosity of the observed FRBs (excluding the recently discovered ASKAP events); and (ii) the Schechter luminosity function. Fialkov et al. showed that if FRBs are standard candles, the contribution of the supercluster is negligible compared to the cosmological contribution within the solid angle of Virgo. However, owing to its proximity, Virgo is expected to dominate the FRB number counts in cases where the faint-end population is numerous (e.g. in the case of a Schechter luminosity function with sufficiently low $L_{\rm min}$ and steep faint-end slope). Assuming that FRB 180417 is outside Virgo, no other FRBs were found in the observed area during the 300 h survey. Using this information, we can provide new limits on the intrinsically faint population of FRBs constraining $L_{\rm min}$ for the first time.

The procedure is as follows. First, we follow the method outlined in Fialkov et al. (2018) to calculate per galaxy FRB event rate based on a cosmological population of FRBs as a function of α and $L_{\rm min}$ and assuming a fixed total rate of $\dot{N}_{\rm FRB} = 10^4$ FRBs per sky per day[3] above the detection threshold of 1 Jy out to redshift $z = 1$ (e.g. Nicholl et al. 2017). Next, we apply this rate to Virgo galaxies extracted from an online Virgo catalogue (Kim et al. 2014) and calculate the expected number of FRBs within the 300 h survey with ASKAP, $\langle N_{\rm FRB}^{\rm Virgo}\rangle$. Finally, we employ Poisson statistics to assess the probability of non-detection of FRBs from Virgo and place limits on α and $L_{\rm min}$.

The cosmic event rate is given by

$$\dot{N}_{\rm FRB} = \int_V {\rm d}V \int_{M_{\rm h}} {\rm d}M_{\rm h} \frac{\rm d}{{\rm d}M_{\rm h}} n(z, M_{\rm h}) \frac{\dot{N}_1(z, M_{\rm h})}{(1+z)} \int_{S>S_{\rm min}} {\rm d}L \left(\frac{L_\nu}{L_{\nu*}}\right)^{-\alpha} \exp\left[-\frac{L_\nu}{L_{\nu*}}\right], \quad (9)$$

where the comoving halo abundance per unit volume (d$n(z, M_{\rm h})$/d$M_{\rm h}$) is calculated using Sheth–Tormen mass function (Sheth & Tormen 1999), the $(1 + z)$ factor accounts for cosmological time dilation and $\dot{N}_1(z, M_{\rm h})$ is the FRB rate per halo. $S_{\rm min}$ is the larger of the telescope sensitivity and the observed flux of the dimmest intrinsic FRB from redshift z, given by $L_{\rm min}(1 + z)/[4\pi D_L^2(z)]$, and $D_L(z)$ is the luminosity distance to the FRB. As in Fialkov et al. (2018), we use two models for the FRB progenitors to relate the per halo rates to the properties of actual galaxies. In the first case, we assume that FRBs trace star formation rate (SFR) and the FRB rate are given by

$$\dot{N}_1(z, M_{\rm h}) = R_{\rm SFR}^{\rm int} \left(\frac{{\rm SFR}(z, M_{\rm h})}{{\rm SFR}_{\rm Virgo}}\right), \quad (10)$$

where $R_{\rm SFR}^{\rm int}$ is the normalization coefficient fixed to yield a total of $\dot{N}_{\rm FRB} = 10^4$ FRBs per sky per day above the detection threshold of 1 Jy out to redshift $z = 1$, SFR$(z, M_{\rm h})$ is the cosmic mean star formation rate in haloes of mass $M_{\rm h}$ at redshift z calculated using the method of Behroozi, Wechsler & Conroy (2013), and ${\rm SFR}_{\rm Virgo} = 776$ M$_\odot$ yr^{-1} is an estimate of the total SFR in Virgo (estimated following Fialkov et al. 2018). In the second scenario, the FRB rate is proportional to the stellar mass M_*:

$$\dot{N}_1(z, M_{\rm h}) = R_{M*}^{\rm int} M_*(z, M_{\rm h})/M_{\rm Virgo}, \quad (11)$$

where $R_{M*}^{\rm int}$ is the normalization coefficient, $M_{\rm Virgo}$ is the total stellar mass in Virgo, $M_{\rm Virgo} \sim 6 \times 10^{12}$ M$_\odot$, and $M_*(z, M_{\rm h})$ is the total stellar mass in a halo of mass $M_{\rm h}$ at redshift z. M_* and $M_{\rm h}$ are related via the star formation efficiency that we also adopt from the work by Behroozi et al. (2013). For a fixed cosmic FRB event rate, the normalization coefficients depend on both α and $L_{\rm min}$ and are shown in Fig. 5 assuming $\dot{N}_{\rm FRB} = 10^4$ FRBs per sky per day.

Next, we identify Virgo galaxies within the observed field (as specified in Fig. 1) using the online Virgo catalogue (Kim et al. 2014). Following Fialkov et al. (2018), for each Virgo galaxy we calculate stellar mass using standard mass–luminosity relations (Bernardi et al. 2010) with luminosities extracted from the catalogue, and the SFR is calculated using the SFR$-M_*$ relation (e.g. Brinchmann et al. 2004). Including all the galaxies located within the field of view, we estimate the total expected number of FRBs from Virgo, $\langle N_{\rm FRB}^{\rm Virgo}\rangle_{\alpha, L_{\rm min}|\dot{N}_{\rm FRB}}$, for a fixed value of $\dot{N}_{\rm FRB}$ and as a function of $L_{\rm min}$ and α using the pre-calculated normalization coefficients, $R_{\rm SFR}^{\rm int}$ and $R_{M*}^{\rm int}$. The predictions are shown in Fig. 5 (right-hand panel) as a function of $L_{\rm min}$ and for three choices of α (1.3, 1.5, 1.7) and for $\dot{N}_{\rm FRB} = 10^4$ FRBs per sky per day with flux >1 Jy and at $z \leq 1$. As anticipated, the lower is $L_{\rm min}$, the more abundant is the population of faint detectable FRBs and the higher is $\langle N_{\rm FRB}^{\rm Virgo}\rangle_{\alpha, L_{\rm min}|\dot{N}_{\rm FRB}}$. The number counts flatten at $L_{\rm min} = 6.4 \times 10^{-6} L_*$ that corresponds to the sensitivity limit of ASKAP. As discussed above, it is likely that the detected FRB is behind Virgo as none of the galaxies from the Virgo Cluster are located close to the line of sight. We estimate the probability to detect zero FRBs from Virgo, $P_0(\alpha, L_{\rm min}|\dot{N}_{\rm FRB})$, as a function of the model parameters using Poisson statistics with the expectation value of $\langle N_{\rm FRB}^{\rm Virgo}\rangle_{\alpha, L_{\rm min}|\dot{N}_{\rm FRB}}$. Because of the high number counts of faint FRBs in the cases with steep luminosity functions and low values of $L_{\rm min}$, the probability for non-detection [the black region in the two-dimensional (2D) probability distribution function (PDF), the top panel of Fig. 6] is low in these cases. Such scenarios are ruled out by the data presented in this paper. On the other hand, in the cases with shallow luminosity function and high values of $L_{\rm min}$ the population is intrinsically bright. As a result, number counts from Virgo are low compared to the yield from the cosmological volume within the field of view. In such cases, it is more likely to find an FRB originating behind Virgo than within the cluster and $P_0(\alpha, L_{\rm min}|\dot{N}_{\rm FRB})$ is high (white region of the 2D PDF, the top panel of Fig. 6).

Marginalizing over one of the parameters we compute one-dimensional (1D) PDFs for the other parameter (lower panels in Fig. 6). Following the indication from Luo et al. (2018) we assume uniform prior on α within 1.2–1.8 and a uniform distribution in $\log_{10} L_{\rm min}$ over the range $[10^{-6}$–$10^{-2}]L_*$. We find that for the total of 10^4 FRBs per sky per day with flux >1 Jy and at $z \leq 1$, the non-detection of FRBs from Virgo is consistent with $\alpha \leq 1.52$ at 68 per cent confidence for both the SFR-driven case and the M_*-driven case. We also find a lower limit on $L_{\rm min}$, with $L_{\rm min} > 7.9 \times 10^{-5} L_* = 1.6 \times 10^{40}$ erg s^{-1} at 68 per cent confidence for the SFR-driven case and with $L_{\rm min} > 9.5 \times 10^{-5} L_* = 1.9 \times 10^{40}$ erg s^{-1} for the M_*-driven case. For 10^3 FRBs per sky per day with flux >1 Jy

[3]Because FRB rates are very uncertain, we also quote the final results for the total of 10^3 FRBs per sky per day above the detection threshold of 1 Jy out to redshift $z = 1$.

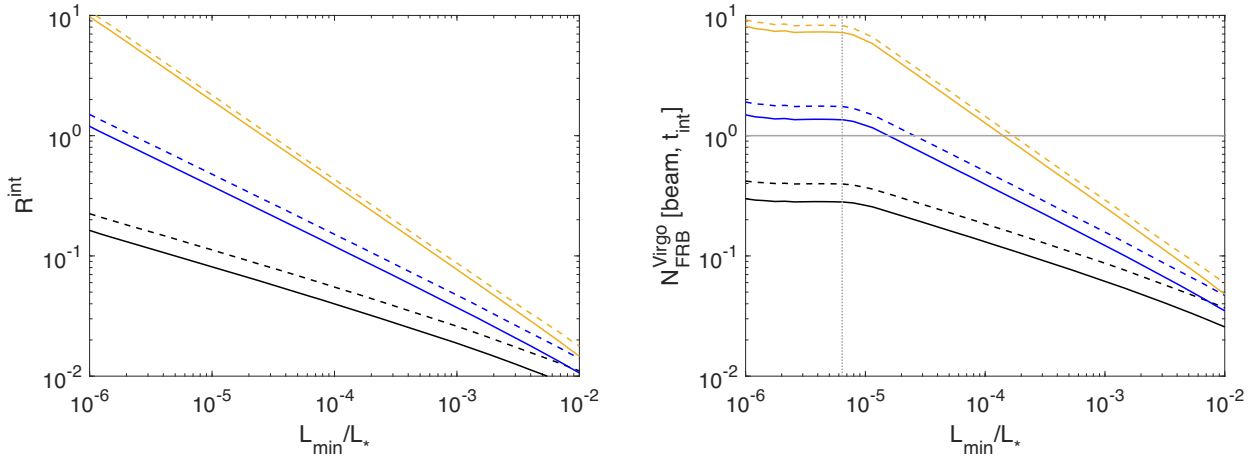

Figure 5. Left: normalization factors, $R^{\rm int}_{\rm SFR}$ (solid) and $R^{\rm int}_{M*}$ (dashed) for Schechter luminosity function with the faint-end slope $\alpha = 1.3$ (black), $\alpha = 1.5$ (blue), $\alpha = 1.7$ (orange) calculated assuming a total of 10^4 FRBs per sky per day above a detection threshold of 1 Jy and out to a redshift of 1. Right: expected total number counts from Virgo within ASKAP field of view over 300 h integration time calculated using the normalization coefficients shown in the left-hand panel. Same colour code is used. The horizontal line shows $\langle N \rangle = 1$ for reference. The vertical dotted line corresponds to the luminosity of the faintest Virgo FRB above the sensitivity limit of ASKAP.

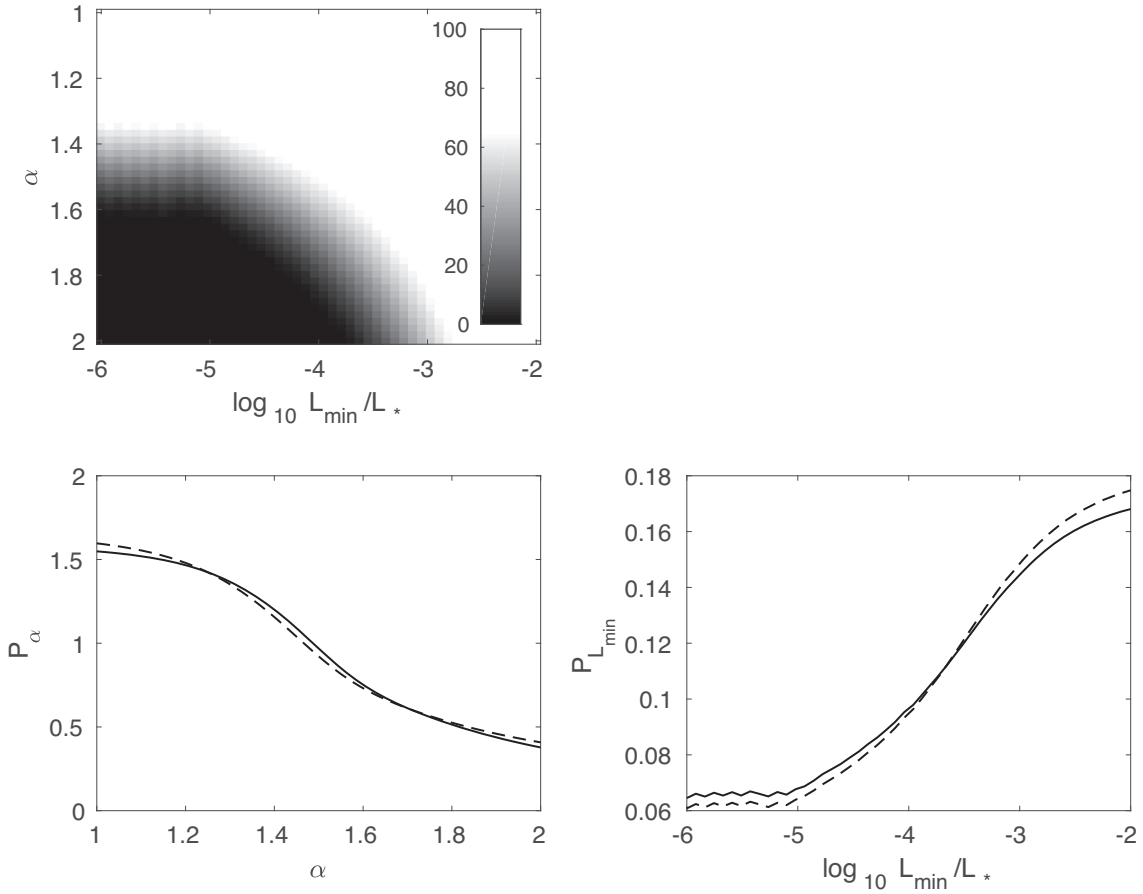

Figure 6. Top: $P_0(\alpha, L_{\rm min}|\dot{N}_{\rm FRB})$, probability of detecting no FRBs from Virgo in 300 h of ASKAP observations as a function of α and $L_{\rm min}$ and assuming the total of 10^4 FRBs per sky per day above a detection threshold of 1 Jy and at $z \leq 1$. Colour code is shown on the colour bar with high probability of non-detection in white and low probability in black. Bottom: one-dimensional (1D) probability distribution functions (PDFs) for α (marginalized over $L_{\rm min}$, left) and $L_{\rm min}$ (marginalized over α, right). The 1D PDFs are shown in the case of the SFR-driven FRBs (solid) and M_* (dashed).

and at $z \leq 1$, the constraints are weaker (because of the lower number counts expected). We find $\alpha \leq 1.58$ and $L_{\rm min} > 4.1 \times 10^{-5} L_* = 6.5 \times 10^{39}$ erg s^{-1} (both at 68 per cent confidence level).

5 CONCLUSIONS

We have presented the discovery and follow-up observations of FRB 180417 from a targeted search of the Virgo Cluster. The search was motivated by the discussion by Fialkov et al. (2018), of possible enhancement in FRB rates in the direction of rich galaxy clusters. The FRB was followed up for 27 h with four more sensitive telescopes at *L* band. No repeat bursts were detected from the target location. We also followed up the FRB in the optical band using the PROMPT5 telescope, but no sources were discovered.

We argue that the FRB is likely behind the Virgo Cluster as the Galactic and intracluster DM contribution was less than the DM of the FRB. Assuming FRB 180417 is beyond Virgo, we constrain for the first time intrinsically faint FRBs ruling out scenarios with a steep faint-end slope of the luminosity function and extremely low values of the minimum intrinsic FRB luminosity. For the total of $\dot{N}_{\rm FRB} = 10^4$ FRBs per sky per day above a threshold of 1 Jy and out to redshift of 1, the minimum luminosity has to be higher than 2×10^{40} erg s^{-1} at 68 per cent confidence level (and higher than 6.5×10^{39} erg s^{-1} for $\dot{N}_{\rm FRB} = 10^3$ FRBs per sky per day). The luminosity function has to be rather shallow with the slope of 1.52 or lower for 10^4 FRBs per sky per day (and of 1.58 or lower for 10^3 FRBs per sky per day).

Our unique limits on the faint-end population of FRBs are enabled solely by the combination of the target cluster search and the large field of view and sensitivity of ASKAP. Blind searches with less sensitive instruments such as the Canadian Hydrogen Intensity Mapping Experiment (CHIME; The CHIME/FRB Collaboration et al. 2019a,b), even though reveal a significant number of new FRBs, are detecting only very bright events. In such searches, the faint-end population remains unconstrained. Further FRB surveys of galaxy clusters with high-sensitivity instruments will shed more light on the minimum intrinsic luminosity of FRBs.

ACKNOWLEDGEMENTS

We thank the anonymous referee for the insightful comments that significantly improved the original manuscript. DA and DRL acknowledge NSF award AAG-1616042. All authors acknowledge support from the NSF awards OIA-1458952 and PHY-1430284. DRL also acknowledges support from the Research Corporation for Scientific Advancement. AF is supported by the Royal Society University Research Fellowship. WF, CF, and RMS acknowledge support through Australian Research Council (ARC) grants FL150100148. RMS acknowledges salary support through grant CE170100004. KWB, J-PM, and RMS acknowledge support through ARC grant DP18010085. GP acknowledges support provided by the Millennium Institute of Astrophysics (MAS) through grant IC120009 of the Programa Iniciativa Cientifica Milenio del Ministerio de Economia, Fomento y Turismo de Chile. SO is supported by the Australian Research Council grant FL150100148. BWS and KR acknowledge support from European Research Council Horizon 2020 grant (no. 694745) during which part of this work was done. DL acknowledges the support from NSFC No. 11725313, No. 11690024, and CAS Strategic Priority Research Program No. XDB23000000. This work was supported in part by the Black Hole Initiative, which is funded by a JTF grant.

The filter bank cut outs for the three beams are available at http://astro.phys.wvu.edu/files/askap_frb_180417.tgz.

REFERENCES

Anantharamaiah K. R., Narayan R., 1988, in Cordes J. M., Rickett B. J., Backer D. C., eds, Proc. AIP Conf. Vol. 174, Radio Wave Scattering in the Interstellar Medium. Am. Inst. Phys., New York, p. 185
Bannister K. W. et al., 2017, ApJ, 841, L12
Bannister K. W. et al., 2019, Science, 365, 565
Becker A., 2015, Astrophysics Source Code Library, record ascl:1504.004
Behroozi P. S., Wechsler R. H., Conroy C., 2013, ApJ, 770, 57
Bernardi M., Shankar F., Hyde J. B., Mei S., Marulli F., Sheth R. K., 2010, MNRAS, 404, 2087
Bertin E., Mellier Y., Radovich M., Missonnier G., Didelon P., Morin B., 2002, in Bohlender D. A., Durand D., Handley T. H., eds, ASP Conf. Ser. Vol. 281, Astronomical Data Analysis Software and Systems XI. Astron. Soc. Pac., San Francisco, p. 228
Binggeli B., Sandage A., Tammann G. A., 1985, AJ, 90, 1681
Brinchmann J., Charlot S., White S. D. M., Tremonti C., Kauffmann G., Heckman T., Brinkmann J., 2004, MNRAS, 351, 1151
Cordes J. M., 1986, ApJ, 311, 183
Cordes J. M., Lazio T. J. W., 2002, preprint (arXiv:astro-ph/0207156)
Cordes J. M., Lazio T. J. W., 2003, preprint (arXiv:astro-ph/0301598)
Dolag K., Gaensler B. M., Beck A. M., Beck M. C., 2015, MNRAS, 451, 4277
Fialkov A., Loeb A., Lorimer D. R., 2018, ApJ, 863, 132
Huchra J. P., Geller M. J., 1982, ApJ, 257, 423
Inoue S., 2004, MNRAS, 348, 999
James C. W., 2019, MNRAS, 486, 5934
James C. W., Ekers R. D., Macquart J.-P., Bannister K. W., Shannon R. M., 2018, MNRAS, 483, 1342
Kim S. et al., 2014, ApJS, 215, 22
Kumar P. et al., 2019, preprint (arXiv:1908.10026)
Li D. et al., 2018, IEEE Microwave Magazine, 19, 112
Lorimer D. R., Bailes M., McLaughlin M. A., Narkevic D. J., Crawford F., 2007, Science, 318, 777
Luo R., Lee K., Lorimer D. R., Zhang B., 2018, MNRAS, 481, 2320
Macquart J.-P. et al., 2010, Publ. Astron. Soc. Aust., 27, 272
Macquart J. P., Shannon R. M., Bannister K. W., James C. W., Ekers R. D., Bunton J. D., 2019, ApJ, 872, L19
Magnier E. A. et al., 2016, preprint (arXiv:1612.05240)
Nan R. et al., 2011, Int. J. Modern Phys. D, 20, 989
Nicholl M., Williams P. K. G., Berger E., Villar V. A., Alexander K. D., Eftekhari T., Metzger B. D., 2017, ApJ, 843, 84
Petroff E. et al., 2016, Publ. Astron. Soc. Aust., 33, e045
Pignata G. et al., 2009, in Giobbi G., Tornambe A., Raimondo G., Limongi M., Antonelli L. A., Menci N., Brocato E., eds, AIP Conf. Proc. Vol. 1111, Probing Stellar Populations Out to the Distant Universe: Cefalu 2008. Am. Inst. Phys., New York, p. 551
Planck Collaboration XL, 2016, A&A, 596, A101
Platts E., Weltman A., Walters A., Tendulkar S. P., Gordin J. E. B., Kandhai S., 2019, Physical Reports, Vol. 821, Elsevier, p. 1
Schinckel A. E., Bunton J. D., Cornwell T. J., Feain I., Hay S. G., 2012, Proc. SPIE, 8444, 84442A
Shannon R. M. et al., 2018, Nature, 562, 386
Sheth R. K., Tormen G., 1999, MNRAS, 308, 119
Smith J. A. et al., 2002, AJ, 123, 2121
Spitler L. G. et al., 2016, Nature, 531, 202
The CHIME/FRB Collaboration et al., 2019a, Nature, 566, 230
The CHIME/FRB Collaboration et al., 2019b, preprint (arXiv:1908.03507)
Thornton D. et al., 2013, Science, 341, 53
Truemper J., 1982, Adv. Space Res., 2, 241
Yao J. M., Manchester R. N., Wang N., 2017, ApJ, 835, 29

This paper has been typeset from a TEX/LATEX file prepared by the author.